Measurement of the Neutron Capture Cross Section of ^{187}W for Production of ^{188}W

Onur Alp Ersöz,[a,b] Robyn Spink,[b,c] Justin R. Griswold,[c*] Fatma Yurt,[a*] Saed Mirzadeh[c]

[a] Department of Nuclear Applications, Institute of Nuclear Science, Ege University, Bornova, 35100, Izmir, Turkey

[b] Department of Nuclear Engineering and Radiological Sciences, University of Michigan, Ann Arbor, MI 48109, United States

[c] Isotopes and Fuel Cycle Technology Division, Oak Ridge National Laboratory (ORNL), Oak Ridge, TN 37831, United States

*Authors for correspondence

Justin R. Griswold: griswoldjr@ornl.gov

Fatma Yurt: ftmyurt@gmail.com

Abstract

Tungsten-188 ($t_{1/2}$ = 69.4 d) is routinely produced by double neutron capture using a highly enriched ^{186}W target, $^{186}W(n,\gamma)^{187}W(n,\gamma)^{188}W$ reaction at ORNL's 85 MWt High Flux Isotope Reactor. While the thermal neutron cross section for the first reaction, $^{186}W(n,\gamma)^{187}W$, is well known, the single reported 64 b cross section for the second reaction, $^{187}W(n,\gamma)^{188}W$, cannot be validated by experimental results that yield lower than expected activities of ^{188}W. In this paper, we report a new value for the thermal neutron capture cross section of ^{187}W. After confirming the neutron capture cross section of ^{186}W (σ^0 = 37.8 ± 1.8 b for thermal; I^0 = 476 ± 25 b for resonance integrals with σ^0/I^0 = 12.6 ± 0.4) in two short irradiations, longer irradiations (1–10 d) were performed to obtain a value of 6.5 ± 0.8 b for the σ^0 of ^{187}W, which is lower than the adopted value by a factor of 10. Due to the short half-life of ^{187}W ($t_{1/2}$ = 23.7 d), the σ^0 for ^{187}W was obtained empirically by comparing the ^{188}W experimental yields with the theoretical yields generated by the IsoChain code and varying the ^{187}W cross section while keeping all other parameters constant.

Keywords; tungsten-187, tungsten-188, neutron capture cross section, neutron-induced nuclear reaction, High Flux Isotope Reactor, HFIR, empirical measurement, IsoChain

1. Introduction

Because of its resistance to high temperatures, tungsten is considered one of the most important structural materials for fusion reactors, and because of its high-density, tungsten is an ideal shielding material for high-energy γ-ray radiation. In addition, tungsten is often used as the target material (i.e., converter) in electron accelerators and fusion reactors for Bremsstrahlung production of photons. An accurate understanding of the thermal neutron cross section and resonance integral for the $^{186}W(n,\gamma)^{187}W$ reaction is critical for calculating the decay heat generated by ^{187}W ($t_{1/2}$ = 23.72 h), affecting reactor design and the evaluation of radiation damage on materials (Naujoks et al., 1996; Al-abyad and Mohamed, 2017). Furthermore, ^{188}W ($t_{1/2}$ = 69.4 d) has an important medical application, as its β^--decay daughter, ^{188}Re ($t_{1/2}$ = 17.0 h), is of considerable interest for various radiotherapeutic applications (Knapp et al., 1997; Jeong and Chung, 2003; Dadachova et al., 2002; Bernal et al., 2007; Pillai et al., 2012; Argyrou et al., 2013).[1] As noted, a major advantage of ^{188}Re is its availability in the carrier-free state from a $^{188}W/^{188}Re$ biogenerator system with a shelf-life of several months. Many therapeutic radionuclides, such as ^{166}Ho ($t_{½}$= 26.8 h) (Dadachova et al., 1994; Zolghadri et al., 2013), ^{177}Lu ($t_{½}$= 6.65 d) (Mirzadeh et al., 2004; Watanabe et al., 2015), ^{153}Sm ($t_{½}$ = 46.3 h) (Mishra et al., 2017) and ^{192}Ir ($t_{½}$ = 73.8 d) (Rostelato et al., 2008), are produced by the (n,γ) reaction in nuclear reactors. W-188, however, is produced through the double neutron capture reaction, $^{186}W(n,\gamma)^{187}W(n,\gamma)^{188}W$. As with other double neutron capture reactions, the product yield is roughly proportional to the square of neutron flux, and efficient production of ^{188}W requires a neutron flux of $\geq 8 \times 10^{14}$ (Argyrou et al., 2013).

The cross section for the first reaction leading to ^{187}W, the intermediate radionuclide, is fairly well known and we have found reasonable agreement with the published and evaluted data which will be discussed later. For the second reaction leading to ^{188}W, $^{187}W(n,\gamma)^{188}W$, the only known cross sections of 64 b (thermal) and 2760 b (resonance integrals) were reported by Gillette (1966). The Gillette report served as an annual report of isotope production activities at ORNL. Unfortunately, no experimental details were given for these measurements except that experiments were conducted at the 10 MW Oak Ridge Research Reactor (ORR, decommisioned in 1987) and that a cadmium filter was used to separate thermal and resonance contributions. Moreover, no uncertainty was reported for the above cross-section values, and the uncertainties of ±10 b (for thermal) and ±550 b (for resonance) listed in current evaluated databases such as Mughabghab (2006) cannot be traced back to the original Gillette report (Garland, 2004). The Gillette report also gives values of 33 b and 318 b for the thermal and resonace cross-sections for the $^{186}W(n,\gamma)^{187}W$ reaction, respectively. However, these values are ~13% and ~34% lower than current adopted values, respectively (see section 3). Later studies documented that large-scale production yields of ^{188}W were lower than theoretical yields by almost one order of magnitude (Knapp et al., 1994; Mirzadeh et al., 1992a). These experiments involved

irradiating several targets consisting of ~50 mg of 96% enriched ^{186}W (as WO_3) in the core of ORNL's HFIR for durations of 1–3 cycles (25–75 days). The very high neutron capture cross section (i.e., burnup cross section) of ^{188}W could also be partly responsible for the discrepancy between the experimental and theoretical yields. The reported burnup cross section of 12.0 ± 2.5 b for ^{188}W (Mirzadeh et al., 1997), however, does not by itself resolve this discrepancy.

In this study, we measured the double neutron capture cross section of ^{186}W leading to ^{188}W via irradiations of several highly enriched ^{186}W targets in HFIR. The first step involved confirming the thermal neutron capture cross section of the $^{186}W(n,\gamma)^{187}W$ reaction through short irradiations. Longer irradiations were then performed to measure the cross section for the $^{187}W(n,\gamma)^{188}W$ reaction. It is important to note that, due to the rather short half-life of ^{187}W, the cross section for the $^{187}W(n,\gamma)^{188}W$ reaction can be evaluated only empirically, by superimposing the experimental ^{188}W yields on the theoretical yield curves while keeping all variables other than the ^{187}W cross section constant.

2. Material and Methods

2.1. ***Irradiation facility.*** HFIR currently operates at an 85 MW power level with near-steady-state thermal neutron fluxes up to 2.1×10^{15} n cm^{-2} s^{-1} and an operating cycle of ~24 days. A hydraulic tube (HT) facility, consisting of a singular bundle of nine aluminum canisters (i.e., "rabbits") that passes through and exits the reactor, provides online access to the core while the reactor is operating. This allows for partial or full-cycle irradiations. Position 5 of the HT facility provides the highest possible thermal neutron flux of 2.1×10^{15} n cm^{-2} s^{-1} with a thermal-to-epithermal flux ratio of 30 (Mirzadeh et al., 1992b). From the center to the top of the core and from the center to the bottom, the thermal neutron flux decreases by a factor of ~2. Detailed information about the neutron flux measurements and neutron spectra unfolding can be found in Mahmood et al. (1995) and Garland et al. (2003). With regard to neutron energy, thermal is defined as E_n = 2200 m/s, epithermal is defined as En ≥ 0.5 eV, and $r = \varphi_{th}/\varphi_{epi}$ is defined as the ratio of the thermal flux to epithermal flux in the energy range 0.5 eV and 0.1 MeV divided by the logarithm of the energy di□erence of that energy range. This term is known as the flux per unit lethargy (see, for example, Hogle et al., 2016; Mirzadeh et al., 2011).

2.2. ***Target preparation and irradiations.*** Tungsten-186, with an isotopic enrichment of 98.44% as tungsten oxide (WO_3), was obtained from the National Isotope Development Center (https://www.isotopes.gov/ibo/ibo.html). The mass distribution of W isotopes in batch 500026, which was used in this study, was as follows: ^{180}W (<0.01%), ^{182}W (0.26 ± 0.01%), ^{183}W (0.22 ± 0.02%), ^{184}W (1.08 ± 0.02%), and ^{186}W (98.44 ± 0.01%). The targets consisted of milligram quantities of enriched ^{186}W oxide, which were encapsulated in high-purity synthetic quartz ampoules (5 mm OD × 3 mm ID × ~20 mm long, Suprasil, Heraeus Amersil, Duluth, GA). The quartz ampoules were cleaned

in concentrated nitric acid, rinsed thoroughly with deionized water and dried at 120°C. Prior to use, the ampoules were allowed to cool to room temperature in a desiccator. The tare weights of each ampoule were recorded after cooling. Tungsten oxide was added to the ampoules, and initial gross weights were measured. The loaded ampoules were placed back in the oven at 120°C for at least 1 h and again allowed the loaded ampoule to cool to room temperature in a desiccator. The final gross weights were used to calculate the net weights of WO_3 in each ampoule (Table 1). The quartz ampoules containing the target material were flame sealed and then placed in aluminum irradiation capsules, welded in a helium atmosphere, and subjected to a helium leak test to ensure weld integrity. A total of five targets were fabricated: two for short irradiations (5 and 55 min) and three for long irradiations (1, 5, and 10 d). The two targets for short irradiations each contained only one glass ampoule, and the three targets for long irradiations each contained two glass ampoules (Table 1). Shorter irradiations were performed at 10% reactor power to reduce the level of ^{187}W activity. The three longer irradiations (>1 day) were conducted at full power. Target masses and irradiations parameter such as irradiation time, neutron flux, and thermal-to-epithermal flux ratios are given in Table 1.

2.3. ***Post irradiation handling of targets.*** After the irradiations, the targets were transferred to a hot cell where the quartz ampoules were removed from the aluminum capsules and after appropriate cooling periods they were transferred to a glovebox. Cooling periods varied; the short irradiation targets were allowed to cool for 3 days, whereas the long irradiation samples were allowed to cool for about 3 weeks. In the glovebox, the ampoules were soaked in concentrated HNO_3 for 5 minutes and rinsed with water to remove any surface contamination. Finally, the samples were either (1) dried and mounted on counting cards for direct activity measurement of ^{187}W or (2) cut open and submerged in 1 mL of 4 M NaOH to dissolve the tungsten oxide. To aid dissolution, the samples were heated to 80–90°C with a hot plate. After dissolution, the sample was evaporated to dryness and then redissolved in a known volume of deionized water. Based on the dose rate and expected activity, the sample was diluted as necessary before assay.

2.4. ***Radioactivity measurements.*** Radioactivity measurements were performed using a calibrated and shielded Canberra Model GC2020 high-purity germanium (HPGe) detector paired with a PC-based multichannel analyzer employing Canberra Genie 2000 software (Canberra Industries, Inc., Meriden, CT). The 100 cm^3 detector has a resolution of 1.0 keV at 123 keV and 1.9 keV at 1332 keV. Energy and efficiency calibrations were determined with γ-ray sources traceable to the National Institute of Standards and Technology. All relevant nuclear data were taken from Firestone and Shirley (1996) and Mughabghab (2006). The half-lives of ^{187}W and ^{188}W, their γ-rays, and their corresponding intensities which were used in this work are summarized in Table 2. Because multiple γ-rays were utilized for assay, the inverse squares of their counting uncertainties were used as weighting factors to calculate the average activity of each sample. Activities were decay-corrected to

obtain the activities at the end of bombardment (EOB), and appropriate corrections were applied to convert the count rates to disintegration rate and to make a small correction due to decay during counting period; $A = (\lambda C)/[(1 - e^{-\lambda t})\varepsilon I_\gamma]$ (1), where A is activity (disintegration per second, dps), C is the uncorrected count rate (counts per second, cps), t is count time (counting period second), λ is the decay constant (1/s), I_γ is γ-ray intensity, and ε is detector efficiency for a specific γ-ray. The activity at EOB per unit mass of target, representing the production yield of the radionuclide, was reported in terms of MBq/mg (i.e., activity of ^{187}W and ^{188}W per gram of ^{186}W target).

2.5. ***Theoretical calculations*.** Theoretical calculations were conducted using the IsoChain code, the JAVA version of its FORTRAN-based predecessor, LAURA (Schmittroth, 2006; Almanza et al., 2006). This code is used to calculate the transmutation and burnup of different nuclei during irradiation (Mirzadeh and Walsh, 1998). IsoChain uses analytical methods to solve the Bateman equations with multiple radionuclides over a user-specified time interval and input flux. Furthermore, IsoChain calculates the production yield of an isotope based on the two-group theory using the thermal and epithermal cross sections and the thermal-to-epithermal neutron flux ratio of the irradiation facility. In this notation, $\sigma_{eff} = \sigma^0 + (1/r)\, I^0$, where $\sigma^0 \equiv$ thermal cross section, $I^0 \equiv$ resonance integrals, and $r = \varphi_{th}/\varphi_{epi}$ (Mirzadeh et al., 2011). The IsoChain input data were determined according to each designed experiment. Input fluxes and flux ratios for each target are given in Table 1.

3. Results and Discussion

Two short irradiations (5 and 55 min, 1 target per time point) were performed to confirm the thermal neutron capture cross section of the ^{186}W(n,γ)^{187}W reaction. Irradiations were performed at a neutron flux of 2.0×10^{14} n cm^{-2} s^{-1} with a thermal to epithermal neutron flux ratio of ~30. These targets were analyzed with no chemical manipulations. As summarized in Table 3, the thermal neutron capture cross sections of the ^{186}W(n,γ)^{187}W reaction for targets 1 and 2 were found to be 37.9 ± 1.4 b and 37.7 ± 2.1 b, respectively, for an average of 37.8 ± 1.8 b. Note that the thermal cross section and resonance integral were not measured independently in this work; rather, these values were calculated from the measured σ_{eff}, the reported ratio of I^0 to σ^0 (12.6 ± 0.43, see Table 3), and a knowledge of thermal to epithermal neutron flux ratios using $\sigma_{eff} = \sigma^0 + (1/r)\, I^0$ (see section 2.5). Neutron self-absorption in tungsten, evaluated by Garland (2004), was found to be negligible for targets with a mass of a few milligrams. The same holds true for absorption of the γ-ray used for the assay of ^{187}W and ^{188}W.

Our measured thermal neutron capture cross-section value for the ^{186}W(n,γ)^{187}W reaction is in good agreement with values reported by Al-abyad and Mohamed (2017), El Abd (2010), and Do et al. (2008), and with the evaluated data of ENDF/B-VII.0 (Chadwick et al., 2006) (Table 3). The cross

sections reported by Garland (2004) and Karadag and Yücel (2004) were slightly higher than this study's results, while cross sections reported by Damle et al. (1967) were slightly lower. The cross section reported by Gillette (1966), at 33 b, is also given in Table 3 for reference.

Three long irradiations (1, 5, and 10 d, two targets per time point) were performed at a neutron flux of ~2 × 10^{15} n cm^{-2} s^{-1} to determine the effective cross section of the $^{187}W(n,\gamma)^{188}W$ reaction (Table 1). These targets were allowed to cool for about 3 weeks and then dissolved. Aliquots of these target solutions were then analyzed. For all six targets, the recovery of radioactivity from the targets was >99%. A typical γ-ray spectrum of a dissolved sample ~60 days post irradiation is shown in Fig. 1a–c. The spectrum shows the counts per channel in the first 2,000 channels, corresponding to ~1000 keV photon energy. While two weak photopeaks of ^{188}W at 227.09 (0.221%) and 290.67 (0.402%) were clearly observable in the presence of the predominant 155.06 keV (14.9%) photopeak from ^{188}Re (Fig. 1a,b), a 15-h count time was necessary to reach ~1% error on the total counts under the ^{188}W photopeaks. Two sets of x-rays in the 59.7–63.0 and 69.3–71.1 keV ranges originates from Re and Os (from β^- decay of ^{188}Re) $K_{\alpha 1,2}$ and $K_{\beta 1\text{-}3}$, respectively (Fig. 1a). The ~1 keV energy resolution of our detector in this energy range is not sufficient to distinguish between Re and Os x-rays. The unlabeled small peaks in Fig. 1c at 322.9, 453.3, 486.1, and 672.5 keV are all in the decay of ^{188}Re, and, with the exception to the 511 keV annihilation peak from background, no other signal can be attributed to any other radioisotope within the ~1000 keV energy range.

Because of the short half-life of ^{187}W, the neutron capture cross section of ^{187}W can only be measured empirically by superimposing experimental data on the theoretical activities for different ^{187}W neutron capture cross-section values while keeping the cross section for the $^{186}W(n,\gamma)^{187}W$ reaction constant. The measured yields, expressed as MBq of ^{188}W per mg of ^{186}W, for 1-, 5-, and 10-day irradiations calculated using equation (1) are given in Table 4. The experimental ^{188}W yields are plotted against the IsoChain-generated yield curves. The production curves were generated by using the thermal neutron capture cross section of 37.8 ± 1.8 b and the resonance integral of 478 ± 25 b (Table 3) for the first reaction and for several thermal cross-section values of 4–64 barns for the second reaction, $^{187}W(n,\gamma)^{188}W$ (Fig. 2a). In this study, we used a value of 43 for the I^0-to-σ^0 ratio (as reported by Gillette, 1966). Using the least-squares technique (Bevington and Robinson, 2003), the best fit between experimental and theoretical yields was obtained with the 6.5 ± 0.8 b cross section with $(I^0/\sigma^0) = 43$ (Fig. 2). The quoted error is derived from the average of relative errors associated with each yield measurement given in Table 4 ($\sigma_{rel} = (1/N)\ SQRT\ [\Sigma\ (\sigma_i/V_i)^2]$). Figure 3 shows the goodness of fit, χ^2, between experimental and theoretical data, which is calculated by the following relationship: $\chi^2 = \Sigma\ \{\sigma_i^{-2}\ [y_i - y(x_i)]^2\}$, where y_i represents the experimentally measured yields and $y(x_i)$ represents the calculated yields for different thermal cross sections, x_i. The approximate location of the minimum can also be calculated by fitting a parabolic function through the χ^2 and solving for the

value of x_i at the minimum. Least-squares treatment of the data gave a value of 6.5 ± 0.2 b (for details, see Bevington and Robinson, 2003, chapter 8). Given that we used a I^0-to-σ^0 ratio based on Gillette's initial measurement, which lacked uncertainties (see section 1), we believe an error of 0.8 or 11% is a more realistic value.

4. Conclusion and Further Studies

In conclusion, our measured values for the neutron capture cross section of ^{186}W (σ^0 = 37.8 ± 1.8 b for thermal; I^0 = 476 ± 25 b for resonance integrals with σ^0/I^0 = 12.6 ± 0.4) are in close agreement with previous studies and adopted values. Results for an empirically measured value for the thermal neutron capture cross section of ^{187}W (6.5 ± 0.8 b) is lower than the adopted value of 64 b by a factor of 10, but it is consistent with the experimental yields obtained from large-scale production of ^{188}W in HFIR.

For further studies, independent measurements of the ^{187}W thermal cross-section and resonance integrals utilizing neutron filters would be very valuable. Due to fast depletion, use of a cadmium filter may be problematic for longer irradiations, but a gadolinium filter could offer a practical alternative.

Acknowledgement. This research was supported by the US Department of Energy, Office of Nuclear Physics, Isotope Program, under contract DE-AC05-00OR22725, and by the Scientific and Technological Research Council of Turkey (TUBITAK) under project number 1059B141600608. The authors acknowledge the efforts and support of the HFIR staff, especially Greg Hirtz for scheduling the irradiations, and staff of ORNL's Nuclear and Radiochemistry Group, Isotope and Fuel Cycle Technology Division, for help in many aspects of this project, especially Allison Peacock and Lance Wyant for handling the irradiated targets in the hot cell. The authors thank James Gaugler II and Riley Hunley, both of ORNL, for their critical review of the manuscript.

References

Al-Abyad, M., Mohamed, G.Y., 2017. Neutron capture cross section measurements and theoretical calculation for the $^{186}W(n,\gamma)^{187}W$ reaction. Radiochim. Acta 105, 347–357.

Almanza, C.L.J., Schmittroth, F., Lovett H.A., Garland M.A., Mirzadeh S., 2006. IsoChain: A user-friendly, two-group nuclear transmutation and decay code. Tran. Am. Nucl. Soc. 95, 441–442.

Argyrou, M., Valassi, A., Andreou, M., Lyra, M., 2013. Rhenium-188 production in hospitals, by W-188/Re-188 generator, for easy use in radionuclide therapy. *Int. J. Mol. Imaging,* Article ID 290750, vol. 2013, https://doi.org/10.1155/2013/29075.

Bernal, P., Raoul, J.L., Stare, J., Sereegotov, E., Sundram, F.X., Kumar, A., Jeong, J.M., Pusuwan, P., Divgi, C., Zanzonico, P., Stare, J., Buscombe, J., Minh, C.T., Saw, M. M., Chen, S., Ogbac, R., Padhy, A.K., 2007. Intra-arterial rhenium-188-labeled lipiodol in the treatment of inoperable hepatocellular carcinoma: Results of an IAEA-sponsored muti-nation study. Int. J. Radiat. Oncol. Biol. Phys. 69, 1448–1455.

Bevington, P.R., Robinson, D.K., 2003. Data Reduction and Error Analysis, 3rd ed., McGraw-Hill, New York.

Chadwick, M.B., et al., 2006. ENDF/B-VII: Next generation evaluated nuclear data library for nuclear science and technology. Nucl. Data Sheets 107, 2931–3060.

Dadachova, E., Mirzadeh, S., Lambrecht, R.M., Hetherington, E.L., and Knapp Jr., F.F. 1994. Separation of carrier-free holmium-166 from neutron irradiated dysprosium targets. Anal. Chem. 66, 4272–4271.

Dadachova, E., Bouzahzah, B., Zuckier, L.S., Pestell, R.G., 2002. Rhenium-188 as an alternative to iodine-131 for treatment of breast tumors expressing the sodium/iodide symporter (NIS). Nucl. Med. Biol. 29, 13–18.

Damle, P.P., Fabry, A., Jacquemin, R., 1967. Study of the reaction $^{186}W(n,\gamma)^{187}W$, Report from Euratom to EANDC-76, 107.

Do, N.V., Khue, P.D., Thanh, K.T., Son, L.T., Kim, G., Lee, Y.S., Oh, Y., Lee, H-S., Cho, M-H., Ko, I.S., Namkung, W., 2008. Thermal neutron cross-section and resonance integral of the $^{186}W(n,\gamma)^{187}W$ reaction. Nucl. Instrum. Meth. *B* 266, 863–871.

El Abd, A., 2010. Measurements of the thermal neutron cross sections and resonance integrals for $^{186}W(n,\gamma)^{187}W$ and $^{98}Mo(n,\gamma)^{99}Mo$ reactions. Radioanal. Nucl. Chem. 284, 321–326.

Firestone, R.B., Shirley, V.S., eds., 1996. Table of Isotopes, 8_{th} ed., John Wiley and Sons Inc., New York.

Garland, M.A., 2004. Neutron Effects on Tungsten-186 Double Neutron Capture. PhD thesis. University of Maryland, College Park. https://drum.lib.umd.edu/handle/1903/1712.

Garland, M.A., Mirzadeh, S., Alexander, C.W., Hirtz, G.J., Hobbs, R.W., Pertmer, G.A., Knapp, F.F., 2003. Neutron flux characterization of a peripheral target position in the High Flux Isotope Reactor. Appl. Radiat. Isot. 59, 63–72.

Gillette J.H., 1966. Review of Radioisotope Program, 1965, Report no. ORNL-4013, Oak Ridge National Laboratory, Oak Ridge, TN, P5.

Hogle, S., Boll, R.A., Murphy, K., Denton, D., Owens, A., Haverlock, T.J., Garland, M., Mirzadeh, S., 2016. Reactor production of thorium-229. Appl. Radiat. Isot. 114, 19–27.

Jeong, J.M., Chung, J.K., 2003. Therapy with ^{188}Re-labeled radiopharmaceuticals: An overview of promising results from initial clinical trials. Cancer Biother. Radiopharm. 18, 707–717.

Karadag, M., Yücel, H., 2004. Measurement of thermal neutron cross-section and resonance integral for $^{186}W(n,\gamma)^{187}W$ reaction by the activation method using a single monitor. Ann. Nucl. Energy 31, 1285–1297.

Knapp Jr., F.F., Callahan, A.P., Beets, A.L., Mirzadeh, S., Hsieh. B.-T., 1994. Processing of reactor-produced tungsten-188 for fabrication of clinical scale alumina-based tungsten-188/Rhenium-188 generators. Appl. Radiat. Isot. 45, 1123–1128.

Knapp Jr., F.F. Beets, A.L., Guhlke, S., Zamora, P.O., Bender, H., Palmedo, H., Biersack, H.J., 1997. Availability of rhenium-188 from the alumina-based tungsten-188/rhenium-188 generator for preparation of rhenium-188-labeled radiopharmaceuticals for cancer treatment. Anticancer Res. 17, 1783.

Mahmood, S.T., Mirzadeh, S., Farrell, K., Pace, J.V., Oliver, B.M., 1995. Neutron Dosimetry of the HFIR Hydraulic Facility, ORNL/TM-12831, Lockheed Martin Energy Systems, Inc., Oak Ridge National Laboratory.

Mirzadeh, S., Knapp Jr., F.F., Callahan, A.P., 1992a. Production of tungsten-188 and osmium-194 in a nuclear reactor for new clinical generators. In Proceedings of the International Conference on Nuclear Data for Science and Technology, Julich, Germany, May 1991, S.M. Qaim, ed., Springer Verlag, New York, 595–597.

Mirzadeh, S., Schenter, R.E., Callahan, A.P., Knapp, F.F., 1992b. Production Capabilities in U.S. Nuclear Reactors for Medical Radioisotopes, Report no. ORNL/TM-12010. Oak Ridge National Laboratory, Oak Ridge, TN.

Mirzadeh, S., Knapp Jr., F.F., Lambrecht, R.M., 1997. Burn-up cross-section of W-188. Radiochim. Acta 77, 99–102.

Mirzadeh, S., Walsh, P., 1998. Numerical evaluation of the production of radionuclides in a nuclear reactor (part 1 & 2). Appl. Radiat. Isot. 49, 379–382, 383–395.

Mirzadeh, S., Du, M., Beets, A.L., Knapp Jr., F.F., 2004. Method for Preparing High Specific Activity ^{177}Lu. US Patent no. 6,716,353.

Mirzadeh, S., Mausner, L.F., Garland, M.A., 2011. Reactor-produced medical radionuclides, in Vertes, A., et al., eds., Handbook of Nuclear Chemistry, second ed., vol. 4, Radiochemistry and Radiopharmaceutical Chemistry in Life Sciences, chapter 38, 1857–1902), Springer, New York.

Mishra, A., Kumar, J., Singh, T., Varde, P.V., Bhattacharya, S., 2017. Production of radioisotopes Sm-153 and Lu-177 in Dhruva. Life Cycle Reliab. Safety Eng. 6, 99–108.

Mughabghab, S.F., 2006. Atlas of Neutron Resonances: Resonance Parameters and Thermal Cross Sections. Z= 1-100, 5th ed. Elsevier, Amsterdam.

Naujoks, D., Asmussen, K., Bessenrodt-Weberpals, M., Deschka, S., Dux, R., Engelhardt, W., Field, A.R., Fussmann, G., Fuchs, J.C., Garcia-Rosales, C., Hirsch, S., Ignacz, P., Lieder, G., Mast, K.F., Neu, R., Radtke, R., Roth, J., Wenzel, U., 1996. Tungsten as target material in fusion devices. Nucl. Fusion 36, 671–686.

Pillai, M.R.A., Dash, A., Knapp Jr., F.F., 2012. Rhenium-188: Availability from the $^{188}W/^{188}Re$ Generator and Status of Current Applications. Curr. Radiopharm. 5, 228–243.

Rostelato, M.E.C.M., Rela, P.R., Zeituni, C.A., Feher, A., Manzoli, J.E., Moura, J.A., Moura, E.S., Silva, C.P.G., 2008. Development and production of radioactive sources used for cancer treatment in Brazil. Nukleonika 53 (suppl. 2), S99−S103.

Schmittroth, F., 2006. "IsoChain: A JAVA-based user-friendly nuclear transmutation and decay code based on FORTRAN code Laura." Unpublished.

Watanabe, S., Hashimoto, K., Watanabe, S., Iida, Y., Hanaoka, H., Endo, K., Ishioka, N.S., 2015. Production of highly purified no-carrier-added ^{177}Lu for radioimmunotherapy. J. Radioanal Nucl. Chem. 303, 935–940.

Zolghadri, S., Jalilian, A.R., Naseri, Z., Yousefnia, H., Bahrami-Samani, A., Ghannadi-maragheh, M., Afarideh, H., 2013. Production, quality control and biological evaluation of ^{166}Ho-PDTMP as a possible bone palliation agent. Iran. J. Basic Med. Sci. 16, 719–725.

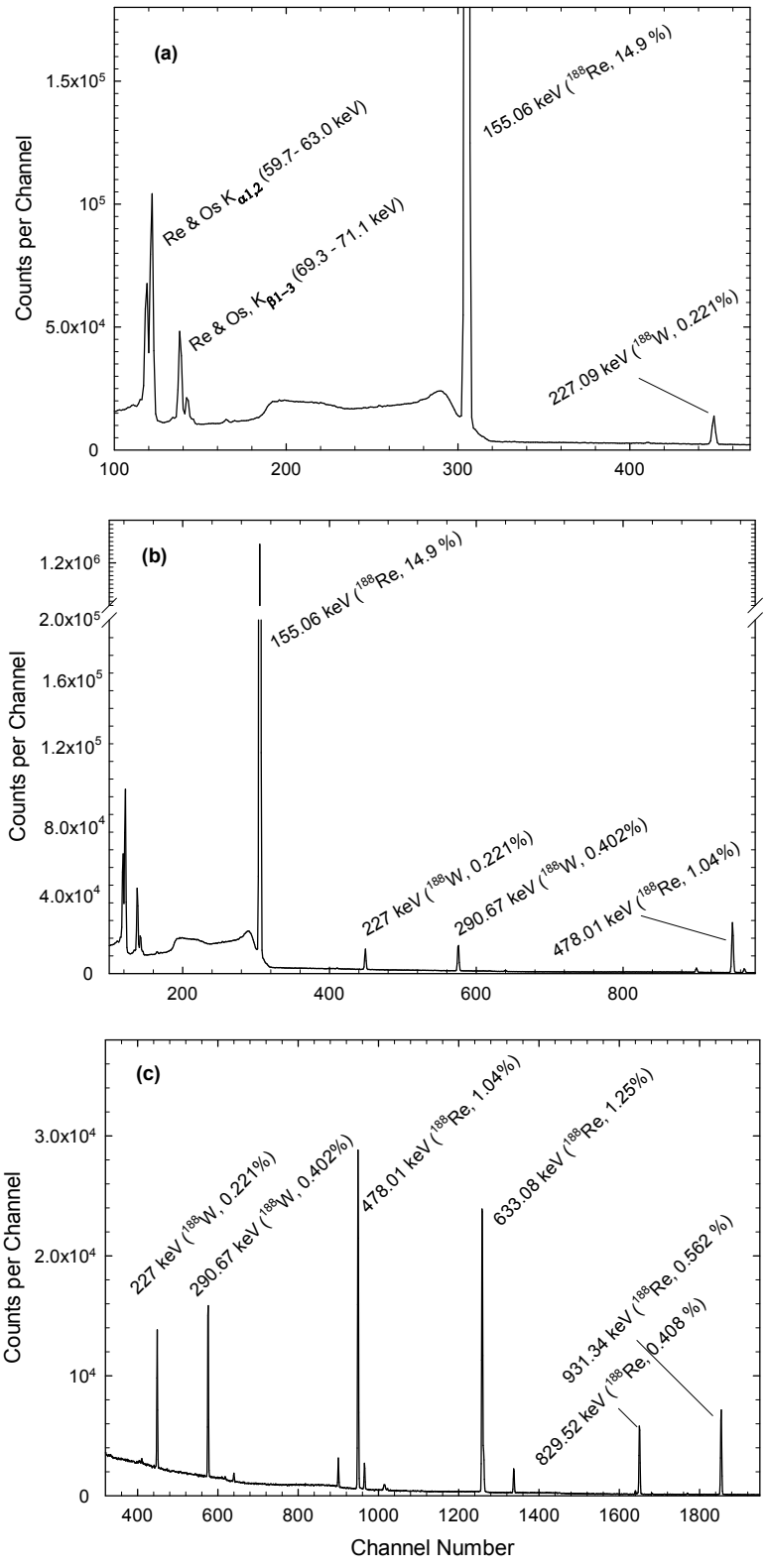
(a)
Counts per Channel
1.5x10^5
10^5
5.0x10^4
0
100
200
300
400
Re & Os Kα1,2 (59.7 - 63.0 keV)
Re & Os, Kβ1-3 (69.3 - 71.1 keV)
155.06 keV (188Re, 14.9 %)
227.09 keV (188W, 0.221%)
(b)
Counts per Channel
1.2x10^6
2.0x10^5
1.6x10^5
1.2x10^5
8.0x10^4
4.0x10^4
0
200
400
600
800
155.06 keV (188Re, 14.9 %)
227 keV (188W, 0.221%)
290.67 keV (188W, 0.402%)
478.01 keV (188Re, 1.04%)
(c)
Counts per Channel
3.0x10^4
2.0x10^4
10^4
0
400
600
800
1000
1200
1400
1600
1800
Channel Number
227 keV (188W, 0.221%)
290.67 keV (188W, 0.402%)
478.01 keV (188Re, 1.04%)
633.08 keV (188Re, 1.25%)
931.34 keV (188Re, 0.562 %)
829.52 keV (188Re, 0.408 %)

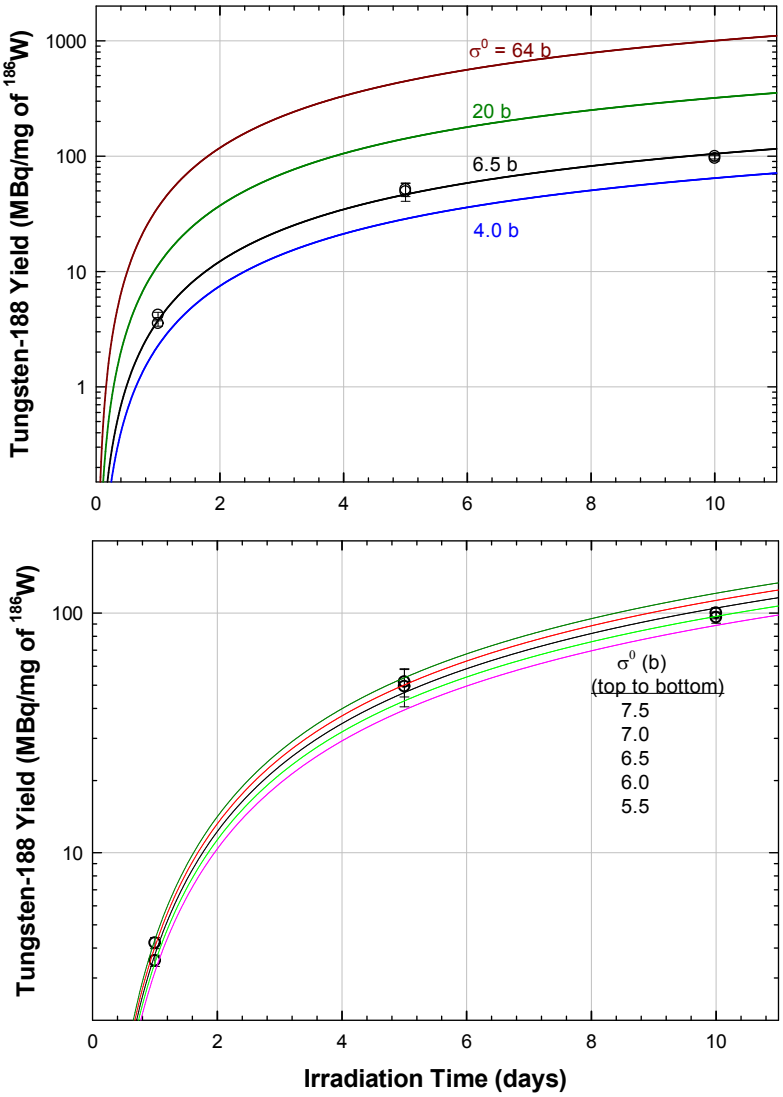
Tungsten-188 Yield (MBq/mg of ^{186}W)
1000
100
10
1
0
2
4
6
8
10
σ^0 = 64 b
20 b
6.5 b
4.0 b
Tungsten-188 Yield (MBq/mg of ^{186}W)
100
10
0
2
4
6
8
10
σ^0 (b)
(top to bottom)
7.5
7.0
6.5
6.0
5.5
Irradiation Time (days)

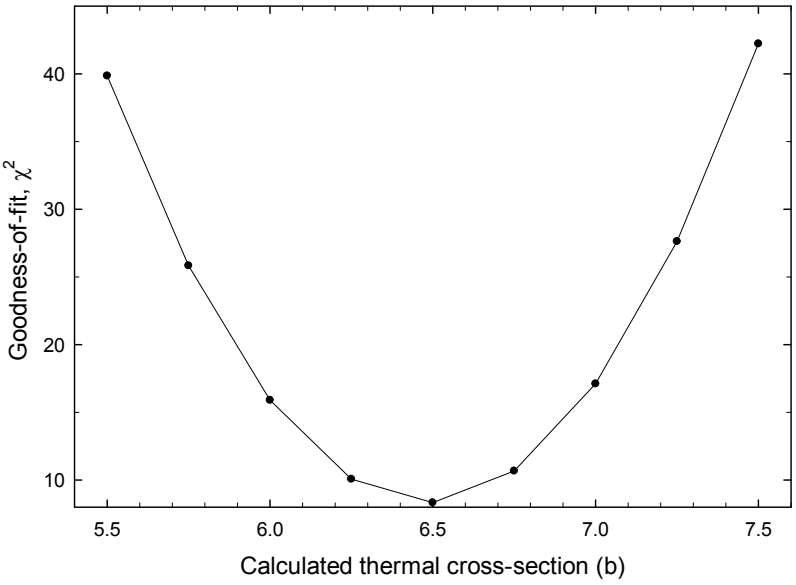
Goodness-of-fit, χ^2
40
30
20
10
5.5
6.0
6.5
7.0
7.5
Calculated thermal cross-section (b)

Captions to the Figures

Figure 1. Gamma-ray spectrum of 69.4-d ^{188}W (target 4a) in full equilibrium with its daughter, 16.98-h ^{188}Re. Data are given for the first 2,000 channels (corresponding to E_γ ~1000 keV). (a) Channels 100-450. (b) Channels 100-900. (c) Channels 360-2000

Spectrum was taken 60 days post-EOB, and sample was counted for 15 h at 30 cm from surface of the HPGe detector with a detector dead time of <1% (see section 2.3). Gamma and x-ray energies and intensities are from Firestone and Shirley (1996).

Figure 2. Experimental and theoretical yields of ^{188}W (MBq/mg) as a function of irradiation time.

Experimental yields are for 1-, 5-, and 10-day irradiation at thermal neutron flux of $\sim 2 \times 10^{15}$ n cm^{-2} s^{-1} with thermal-to-epithermal neutron ratios of 30 (see Table 1). Uncertainties of the data points are about the size of the markers or smaller. (a) Theoretical ^{188}W yield curves (solid lines) are for 64 b, 20 b, 6.5 b, and 4.0 b for cross section of ^{187}W(n,γ)^{188}W reaction at the same neutron fluxes. (b) Theoretical ^{188}W yield curves (solid lines) for 5.5–7.5 b.

Figure 3. Plot of goodness of fit, chi-square, as a function of IsoChain-generated thermal neutron cross-sections.

Location of the minimum is calculated by fitting a parabola through nine calculated points (5.5–7.5 b) closer to the minimum (6.5 b).

Table 1. Experimental irradiation parameters for target material

Target no.	^{186}W mass (mg)	Irradiation time	HFIR HT position	φ_0 [a] (n cm^{-2} s^{-1})
1	18.23	5 min	5	2.0×10^{14}
2	1.97	55 min	5	2.0×10^{14}
3a	7.89	1 d	4	2.0×10^{15}
3b	7.34	1 d	4	2.0×10^{15}
4a	7.37	5 d	6	1.95×10^{15}
4b	10.3	5 d	6	1.95×10^{15}
5a	7.65	10 d	4	2.0×10^{15}
5b	8.37	10 d	4	2.0×10^{15}

[a] With a thermal to epithermal neutron flux ($r = \varphi_{th}/\varphi_{epi}$) ~30; HT = hydraulic tube

Table 2. Half-lives of ^{187}W, ^{188}W, and ^{188}Re, their γ-rays, and γ-ray intensities used in this study[a]

Radio-nuclide	Half-life	γ-ray used for assay ^{187}W and ^{188}W	
		Energy (keV)	**Intensity** (%)
^{187}W	23.7 ± 0.1 d	134.25 ± 0.01	8.85 ± 0.16
		479.55 ± 0.02	21.8 ± 0.4
		551.52 ± 0.04	5.08 ± 0.11
		685.74 ± 0.02	27.3 ± 0.6
		772.89 ± 0.04	4.12 ± 0.08
^{188}W	69.4 ± 0.5 d	227.09 ± 0.02	0.221 ± 0.008
		290.67 ± 0.01	0.402 ± 0.012
^{188}Re	16.98 ± 0.02 h	155.03 ± 0.01	14.95 ± 0.51
		477.99 ± 0.02	1.01 ± 0.03
		632.98 ± 0.02	1.25 ± 0.04
		829.46 ± 0.03	0.403 ± 0.011
		931.34 ± 0.02	0.545 ± 0.020

[a] Data from Firestone and Shirley (1996)

In addition to 227.1 and 290.7 keV γ-rays from ^{188}W, 5 γ-rays from ^{188}Re (in full equilibrium with ^{188}W) were used for the assay of ^{188}W. In this case, intensities of ^{188}Re γ-rays were multiplied by 1.013, corresponding to the ratio of $\lambda_2/(\lambda_2 - \lambda_1)$, where λ_1 and λ_2 represent the ^{188}W and ^{188}Re decay constants, respectively.

Table 3. Thermal neutron cross section for $^{186}W(n,\gamma)^{187}W$ reaction

Measurements	Irradiation facility	Neutron capture cross section (b)		σ^0/I^0
		Thermal, σ^0	Resonance Integrals, I^0	
This work[a]				
Target 1	Reactor	37.9 ± 1.4	478 ± 24	
Target 2		37.7 ± 2.1	475 ± 26	
Average		37.8 ± 1.8		
Evaluated nuclear data				
ENDF/B or Mughabghab (2006)		38.1 ± 0.5	480 ± 15	12.6 ± 0.4
Other measurements				
Al-abyad and Mohamed (2017)	Reactor	39.1 ± 2.6	419 ± 74	10.7 ± 2.0
	Am-Be	38.8 ± 1.0	439 ± 36	11.3 ± 1.0
El Abd (2010)	Reactor	38.4 ± 0.4	502 ± 65	13.2 ± 2.2
Do et al. (2008)	Linac	37.2 ± 2.1	461 ± 39	12.4 ± 1.3
Karadag et al. (2004)	Am-Be	39.5 ± 2.3	493 ± 40	12.5 ± 1.3
Garland et al. (2003)	Reactor	43.5 ± 4.0	395 ± 32	9.1 ± 1.1
Damle et al. (1967)	Reactor	35.4 ± 0.8	534 ± 50	15.1 ± 1.5
Gillette (1966)	Reactor	33	318	9.6

[a] Thermal cross section (σ^0) and resonance integral (I^0) were calculated from the measured σ_{eff} and the reported I^0-to-σ^0 ratio of 12.6 ± 0.4 (see section 3).

Table 4. Experimental activities of ^{188}W at EOB

Target no.	Experimental activities of ^{188}W at EOB (MBq/mg of ^{186}W)
3a	4.1 ± 0.8
3b	3.3 ± 0.8
4a	52 ± 3
4b	49 ± 3
5a	96 ± 6
5b	100 ± 6

EOB = end of bombardment